

Received September 13, 2020, accepted September 16, 2020, date of publication September 18, 2020, date of current version September 29, 2020.

Digital Object Identifier 10.1109/ACCESS.2020.3024573

Robust Satellite Formation Flying Controller Design Subject to Communication Delays

YUE GAO¹, HAO LIU^{1,2,3} (Member, IEEE), AND YU TIAN^{2,3}

¹Space Star Technology Company, Ltd., Beijing 100086, China

²School of Astronautics, Beihang University, Beijing 100191, China

³Key Laboratory of Spacecraft Design Optimization and Dynamic Simulation Technologies of Ministry of Education, Beihang University, Beijing 100191, China

Corresponding author: Hao Liu (liuhao13@buaa.edu.cn)

This work was supported by the National Natural Science Foundation of China under Grant 61873012 and Grant 61503012.

ABSTRACT A robust control method is proposed to address the satellite formation flying problem subject to communication delays. Each satellite dynamics involves nonlinear dynamics, parametric uncertainties, and external disturbances. Communications between neighboring satellites are affected by time delays. For each satellite, the resulted controller includes a translational controller to maintain the desired formation pattern, and a rotational controller to align the attitude. Theoretical analysis and simulation results are provided to verify the advantages of the proposed formation flying controller.

INDEX TERMS Formation control, robust control, nonlinear system, uncertain system, satellite.

I. INTRODUCTION

Satellite formation flying is a timely and challenging problem in aerospace. Compared to a traditional single satellite or complex spacecraft, satellite formation flying can effectively improve overall system performance, and has multiple advantages: high reliability, flexibility, and low cost. As such, there are broad application prospects related to deep space exploration, near-earth surveillance, and commercial communication, as shown in [1]–[3]. However, there exist challenges in the design of the satellite distributed formation controller, because each satellite dynamics involves nonlinear dynamics, parametric uncertainties, and external disturbances. The parameter of inertia can be perturbed because of the satellite on-board fuel consumption, and unknown external disturbances such as the Earth's non-spherical gravity and solar radiation pressure. Third body gravity can also influence the formation flying controller. An additional challenge relates to the communication between neighboring satellites, which introduces time delays that can degrade the formation control performance and affect the stability of the global closed-loop control system.

Previous results on the centralized formation control problem have been reported in [4]–[8]. In [4], a simplified linear motion was used to describe satellite dynamics, and a linear system control algorithm for satellite formation flying was

introduced. In [5], a filter based on variable structure control concept was presented for satellite attitude synchronization. In [6], a relative position keeping problem in satellite formation flying was studied, and a composite nonlinear feedback controller was established by using an algebraic Riccati inequality and a low-and-high gain control strategy. In [7], the formation control problem for a team of tethered satellites actuated by reaction wheels and electromagnetic dipoles was investigated, and a robust sliding mode controller was designed for both translational and rotational dynamics. However, for these designed centralized formation control methods, the resulted centralized control structure introduces requirements for the communication network bandwidth, as shown in [4]–[8].

Moreover, considerable works have been done on the distributed control methods of satellite formation flying, while undirected and directed graphs have been used to design the distributed formation control protocol. Based on the undirected graph approach, a suboptimal distributed controller using linear matrix inequalities was designed in [9], and a distributed optimal formation algorithm was studied in [10] to solve the spacecraft formation control problem. Undirected communication requires that each satellite can receive and send information, while directed communication can reduce requirements for communication equipment and links among satellites. Satellite formation flying controllers based on the directed graph approach were discussed in [11]–[14]. Distributed cooperative attitude synchronization and tracking

The associate editor coordinating the review of this manuscript and approving it for publication was Jianyong Yao ¹.

problems were discussed in [11], but the influence from uncertainties and disturbances on the global system was ignored. Considering parametric uncertainties and external disturbances, distributed controllers were developed based on an adaptive control architecture in [12], while a bounded output feedback control protocol was constructed in [13], and a robust formation controller was designed in [14] and [15]. However, the effects of the communication delays between neighboring satellites were ignored in the stability analysis of the aforementioned controller design methods, as shown in [9]–[15].

Due to the limitation of communication equipment and distance, there usually exist time delays in the process of information transmission among satellites. The influence of time delays on satellite formation control systems were considered in [16]–[18]. In the presence of external disturbances and communication time delays, a sliding mode control strategy was designed in [16] to achieve the spacecraft formation flying. The attitude control problem for satellite formation with time delays was discussed in [17]. However, the control protocol designed in [16] and [17] were based on the undirected graph. In [18], the attitude synchronization control problem for spacecraft formation flying with communication delays was dealt with, but the implementation of the controller required a known amount of time delay and only external constant perturbations were considered. However, the disturbance rejection problems subject to nonlinear dynamics, multiple uncertainties, and communication delays simultaneously were not further studied by these control methods, as shown in [16]–[18].

It is challenging to design robust formation controller for a group of satellites with communication delays when the dynamics of each satellite involve nonlinearities and uncertainties in both the position and attitude motions. First, simplified dynamic models in [4] were used to describe the satellite motion, but it is not accurate enough in complex aerospace. The trajectory formation and attitude coordination problems were discussed separately in [5], [19]. Second, uncertainty rejection problems were ignored in satellite formation control problems reported in [11], [20], and limited types of uncertainties were discussed in stability analysis of the constructed global closed-loop control systems as shown in [12], [20]. An on-line parameter adaptation and a robust control law are involved in [21] which were used to handle the matched parametric uncertainty and the matched disturbance. An output feedback robust controller is proposed by integrating an extended state observer and a novel robust controller in [22] with which one can estimate the unmeasurable system states and the additive disturbances only with the output measurement and delayed control input. However, the effects of the communication delays between neighboring satellites were ignored in the stability analysis of the aforementioned papers. The effects of the communication delays between neighboring satellites were also ignored in the stability analysis in [3]–[5], [11]–[14]. Therefore, robust formation control for

a group of satellites considering communication delays is still open.

Therefore, to the best of the authors' knowledge, the problem to restrain multiple uncertainties and communication delays on the global satellite formation control system is still challenging, while the communication is described by the directed graph and multiple uncertainties include nonlinear dynamics, parametric uncertainties, and external disturbances. In this article, the robust control problem for satellite formation flying subject to communication delays is addressed. Compared to previously published papers, the new contributions in the current manuscript can be illustrated as follows:

First, each satellite dynamics includes nonlinear dynamics, parametric uncertainties, and time-varying external disturbances. It is proven that the translational and rotational tracking errors of the global nonlinear and uncertain control system can converge into a given neighborhood of the origin in a finite time. However, the nonlinear dynamics of the satellites in the formation was simplified in [19], and the disturbance rejection problems were not further addressed in [20].

Second, the influence of the communication delays between neighboring satellites on the global uncertain closed-loop control system can be restrained, simultaneously. The communication time delays and the uncertainties involving parametric perturbations and external disturbances are included in the equivalent disturbances, and a robust compensating control input based on the signal compensation theory is introduced to counteract the effects of the equivalent disturbances on the global system. However, the effects of the communication delays were not fully studied in [3], for the global uncertain satellite formation flying system.

Third, the communication topology among satellites is described by the directed graph, and the resulted satellite formation controller is distributed. For each satellite, the resulted formation controller only depends on the state information from itself and its neighbors. But, the distributed formation control problems were not further studied in [18].

The outline of this article is shown as follows. The problem formulation including the graph theory, satellite model description, and control objectives is introduced in section II. The robust formation controller for the satellite group is designed in section III. IV and V describe the robustness properties and simulation results, respectively. VI concludes the whole work.

II. PROBLEM FORMULATION

A. GRAPH THEORY

To describe the communication topology among finite homogeneous satellites in the formation, a basic knowledge of the graph theory is introduced here. Let $\Phi = \{1, 2, \dots, N\}$ and the satellites are numbered from 1 to N . Denote $G = \{V, E\}$ as a directed graph with $V = \{v_1, v_2, \dots, v_N\}$ a finite set of nodes and $E \in \{(v_i, v_j) : v_i, v_j \in V\}$ a finite set of edges.

Node v_i represents satellite i and an edge $(v_i, v_j) \in E$ the information can flow from satellite i to satellite j . Define a connectivity matrix $A = [a_{ij}] \in \mathbb{R}^{N \times N}$. The element a_{ij} is positive, if $(v_j, v_i) \in E$; $a_{ij} = 0$, otherwise. Besides, $a_{ii} = 0$. Denote the in-degree of node v_i as $d_i(v_i) = \sum_{j=1}^N a_{ij}$, and $D = \text{diag}\{d_i(v_i)\} \in \mathbb{R}^{N \times N}$ the in-degree matrix. The graph Laplacian matrix is defined as $L = D - A$. If there is a directed path from a node to every other node, the graph has a spanning tree and the node is called the root of the tree.

Notations: Denote $I_N \in \mathbb{R}^{N \times N}$ as an identity matrix, $c_{N,j} \in \mathbb{R}^{N \times 1}$ a column vector with all 0 except for 1 on the j -th element, $0_{a \times b} \in \mathbb{R}^{a \times b}$ a zero matrix, s the Laplace operator, and \otimes the Kronecker product. Define a skew-symmetric matrix $S(\cdot)$ for a vector $b = [b_1 \ b_2 \ b_3]^T \in \mathbb{R}^{3 \times 1}$ as:

$$S(b) = \begin{bmatrix} 0 & -b_3 & b_2 \\ b_3 & 0 & -b_1 \\ -b_2 & b_1 & 0 \end{bmatrix}.$$

B. MODEL DESCRIPTION

In this article, the leader satellite can be considered as a virtual leader for the group of satellites and follows a circular reference orbit. Let $\hat{E}_I = \{\hat{e}_x^I, \hat{e}_y^I, \hat{e}_z^I\}$ denote an Earth-fixed inertial frame, $\hat{E}_M = \{\hat{e}_x^M, \hat{e}_y^M, \hat{e}_z^M\}$ a leader satellite-fixed frame attached to its mass center, and $\hat{E}_{Bi} = \{\hat{e}_{xi}^B, \hat{e}_{yi}^B, \hat{e}_{zi}^B\}$ a body-fixed frame rigidly attached to satellite i . As shown in [12], for satellite i , the relative translational dynamics can be modeled as follows:

$$\begin{aligned} \ddot{p}_{xi} &= \omega_{0L}^2 p_{xi} + 2\omega_{0L} \dot{p}_{xi} + \mu_g / r_{0L}^2 + u_{xi} + d_{xi} \\ &\quad - \mu_g (r_{0L} + p_{xi}) / r_i^3, \\ \ddot{p}_{yi} &= \omega_{0L}^2 p_{yi} - 2\omega_{0L} \dot{p}_{xi} - \mu_g p_{yi} / r_i^3 + u_{yi} + d_{yi}, \\ \ddot{p}_{zi} &= -\mu_g p_{zi} / r_i^3 + u_{zi} + d_{zi}, \end{aligned} \quad (1)$$

where $p_i = [p_{xi} \ p_{yi} \ p_{zi}]^T \in \mathbb{R}^{3 \times 1}$ represents the relative translational position in \hat{E}_M and $u_{ti} = [u_{xi} \ u_{yi} \ u_{zi}]^T \in \mathbb{R}^{3 \times 1}$ the relative control acceleration vector. $\omega_{0L} = \sqrt{\mu_g / r_{0L}^3}$ indicates the orbital angular velocity of the leader satellite, μ_g the Earth's gravitational constant, r_{0L} the leader satellite's orbit radius, $r_i = \sqrt{(r_{0L} + p_{xi})^2 + p_{yi}^2 + p_{zi}^2}$ the distance between satellite i and Earth, and $d_{pi} = [d_{xi} \ d_{yi} \ d_{zi}]^T \in \mathbb{R}^{3 \times 1}$ the acceleration caused by external disturbances including the Earth's non-spherical gravity, solar radiation pressure, and third body gravity. Most of the parameters of the subscript represent the dynamic parameters of a single satellite, and the dimension is 3×1 .

The attitude kinematics for a rigid satellite i can be described by modified Rodrigues parameters (MRPs) as

$$\dot{\sigma}_i = H(\sigma_i) \omega_i, \quad (2)$$

where $\sigma_i = [\sigma_{1i}, \sigma_{2i}, \sigma_{3i}]^T$ is a parameter vector, $\omega_i = [\omega_{xi} \ \omega_{yi} \ \omega_{zi}]^T \in \mathbb{R}^{3 \times 1}$ the angular velocity vector in \hat{E}_{Bi} , $H(\sigma_i) = ((1 - \sigma_i^T \sigma_i)I_3 + 2\sigma_i \sigma_i^T + 2S(\sigma_i)) / 4$ an invertible

matrix. The rotational dynamics for satellite i can be written as

$$J_i \dot{\omega}_i = -S(\omega_i) J_i \omega_i + \tau_i + d_{\tau i}, \quad (3)$$

where $J_i = \text{diag}\{J_{xi}, J_{yi}, J_{zi}\} \in \mathbb{R}^{3 \times 3}$ is the inertia matrix of each satellite, $\tau_i = [\tau_{xi} \ \tau_{yi} \ \tau_{zi}]^T \in \mathbb{R}^{3 \times 1}$ the internal control torque, and $d_{\tau i} = [d_{\tau xi} \ d_{\tau yi} \ d_{\tau zi}]^T \in \mathbb{R}^{3 \times 1}$ the external disturbances. By combining (2) and (3), one can obtain that the Lagrangian expression with respect to MRPs as:

$$M(\sigma_i) \ddot{\sigma}_i + C(\sigma_i, \dot{\sigma}_i) \dot{\sigma}_i = u_{\tau i} + H(\sigma_i)^{-1} d_{\tau i}, \quad (4)$$

where $u_{\tau i} = H^{-1}(\sigma_i) \tau_i$ is defined as the torque control input, $M(\sigma_i) = H^{-1}(\sigma_i) J_i H^{-1}(\sigma_i)$, and $C(\sigma_i, \dot{\sigma}_i) = H^{-1}(\sigma_i) (J_i \dot{H}(\sigma_i) + S(H(\sigma_i) \dot{\sigma}_i) J_i H(\sigma_i))$. From (1) and (4), one can see that the translational and the rotational models are highly nonlinear. Altitude and size of flying agents can affect the model parameters of these agents which have great influence on the controller design.

C. PROBLEM DESCRIPTION

In this article, the control objectives for the satellite group are to form desired time-varying formation patterns and trajectories, and achieve the satellite attitude consensus. Denote ζ_{pij} and $\zeta_{\sigma ij} (i, j \in \Phi)$ as the desired translational and rotational deviations between satellite i and satellite j , respectively. Let $p^r \in \mathbb{R}^{3 \times 1}$ and $\sigma^r \in \mathbb{R}^{3 \times 1}$ represent the desired trajectory and attitude of the virtual leader, and assume that the second derivatives of p^r and σ^r satisfy $\ddot{p}^r = 0$ and $\ddot{\sigma}^r = 0$. Let $\zeta_{pij} = \zeta_{pi} - \zeta_{pj}$ and $\zeta_{\sigma ij} = \zeta_{\sigma i} - \zeta_{\sigma j} (i, j \in \Phi)$, where ζ_{pi} and $\zeta_{\sigma i}$ indicate the desired translational and rotational deviations between the leader satellite and satellite i , and $\sum_{i=1}^N \zeta_{pi} = 0_{3 \times 1}$. In order to make all satellites reach a consistent attitude, $\zeta_{\sigma ij}$ is set to be $0_{3 \times 1}$ and thus $\zeta_{\sigma i} = 0$.

To analyze the robust control problem, the real parameter of the satellite motion model can be divided into two parts: one is the nominal part expressed by superscript N , the other is the uncertain part expressed by superscript Δ . Therefore, for example, $J_i = J_i^N + J_i^\Delta$ and $M(\sigma_i) = M^N(\sigma_i) + M^\Delta(\sigma_i)$. The parametric uncertainties are bounded and satisfy $\|M^{-1}(\sigma_i) M^\Delta(\sigma_i)\|_1 < 1$. The feedback linearization control scheme is first applied to the satellite translational model (1) and the rotational model (4). Design the virtual translational and rotational control inputs $u_{pi} = [u_{pxi} \ u_{pyi} \ u_{pzi}]^T \in \mathbb{R}^{3 \times 1}$ and $u_{\sigma i} = [u_{\sigma 1i} \ u_{\sigma 2i} \ u_{\sigma 3i}]^T \in \mathbb{R}^{3 \times 1}$ to cancel nonlinearities as:

$$\begin{aligned} u_{pxi} &= \ddot{p}_{xi} - \mu_g (r_{0L} + p_{xi}) / r_i^3 + \mu_g / r_{0L}^2, \\ u_{pyi} &= \ddot{p}_{yi} - \mu_g p_{yi} / r_i^3, \\ u_{pzi} &= \ddot{p}_{zi} - \mu_g p_{zi} / r_i^3, \\ u_{\sigma i} &= M^N(\sigma_i)^{-1} (u_{\tau i} - C^N(\sigma_i, \dot{\sigma}_i) \dot{\sigma}_i). \end{aligned} \quad (5)$$

Then the satellite motion (1) and (4) can be rewritten as

$$\begin{aligned} \ddot{p}_i &= C_{p1i}^N \dot{p}_i + C_{p2i}^N p_i + u_{pi} + \Delta p_i, \\ \ddot{\sigma}_i &= u_{\sigma i} + \Delta \sigma_i, \quad i \in \Phi, \end{aligned} \quad (6)$$

where

$$C_{p1i}^N = \begin{bmatrix} 0 & 2\omega_{0L} & 0 \\ -2\omega_{0L} & 0 & 0 \\ 0 & 0 & 0 \end{bmatrix},$$

$$C_{p2i}^N = \begin{bmatrix} \omega_{0L}^2 & 0 & 0 \\ 0 & \omega_{0L}^2 & 0 \\ 0 & 0 & 0 \end{bmatrix}.$$

$\Delta_{pi} \in \mathbb{R}^{3 \times 1}$ and $\Delta_{\sigma i} \in \mathbb{R}^{3 \times 1}$ in (6) represent equivalent disturbances, involving parametric perturbations and external disturbances, which we're dealing with to restrain the effects, and satisfy the following equations

$$\begin{aligned} \Delta_{pi} &= d_{pi}, \\ \Delta_{\sigma i} &= M^{-1}(\sigma_i)H^{-1}(\sigma_i)d_{\tau i} \\ &\quad - M^{-1}(\sigma_i)M^\Delta(\sigma_i)u_{\sigma i} \\ &\quad - M^{-1}(\sigma_i)C^\Delta(\sigma_i, \dot{\sigma}_i)\dot{\sigma}_i. \end{aligned} \quad (7)$$

The external disturbances d_{pi} and $d_{\sigma i}$ are assumed to be bounded.

Remark 1: It can be observed from (6) that the real motion model of the satellite includes a nominal model and the equivalent disturbances. In fact, the satellite model (6) can be regarded as the nominal model by ignoring the equivalent disturbances Δ_{pi} and $\Delta_{\sigma i}$.

III. FORMATION CONTROLLER DESIGN

In this section, a formation controller is proposed for the satellite group, which includes a translational formation controller to form the desired formation patterns and track the desired trajectories, and a rotational formation controller to make the satellite attitude consensus.

A. TRANSLATIONAL FORMATION CONTROLLER DESIGN

The translational control input $u_{pi}(t)$ for satellite i is designed as:

$$u_{pi}(t) = u_{pi}^N(t) + u_{pi}^R(t), \quad i \in \Phi, \quad (8)$$

where $u_{pi}^F \in \mathbb{R}^{3 \times 1}$ is the nominal part for the nominal model to achieve desired tracking properties, and $u_{pi}^R \in \mathbb{R}^{3 \times 1}$ is the robust compensating part to restrain the effects of Δ_{pi} in (6) on the closed-loop control system. It should be noted that there exists a communication delay h when satellite i receives information from its neighbors. The communication delays are nonnegative and assumed to be uniformly bounded functions, satisfying $\bar{h} = \max \|h\|_\infty < \infty$ and $\bar{h}_d = \max \|\dot{h}\|_\infty < 1$. In this case, by ignoring the equivalent disturbance Δ_{pi} , the nominal translational control input u_{pi}^N can be designed to achieve desired translational tracking properties as:

$$\begin{aligned} u_{pi}^F &= -\alpha_F \sum_{j \in N} a_{ij}K_p(p_i(t) - p_j(t-h) - \zeta_{pi}) \\ &\quad - \alpha_F \sum_{j \in N} a_{ij}K_{\dot{p}}(\dot{p}_i(t) - \dot{p}_j(t-h) - \dot{\zeta}_{pi}) \end{aligned}$$

$$\begin{aligned} &-\alpha_F \beta_{li}K_p(p_i(t) - \zeta_{pi} - p^r(t)) \\ &-\alpha_F \beta_{li}K_{\dot{p}}(\dot{p}_i(t) - \dot{\zeta}_{pi} - \dot{p}^r(t)), \end{aligned} \quad (9)$$

where $\alpha_F \in \mathbb{R}^{1 \times 1}$ represents a scalar coupling gain, β_{li} is a constant indicating the connection between the virtual leader and satellite i . When $\beta_{li} = 1$, the virtual leader can transmit information to satellite i , otherwise $\beta_{li} = 0$. $K_p, K_{\dot{p}} \in \mathbb{R}^{3 \times 3}$ are diagonal nominal controller parameter matrices to be determined. Define $M_p = M_p^T \in \mathbb{R}^{6 \times 6}$ and $\Pi_p = \Pi_p^T \in \mathbb{R}^{3 \times 3}$ are symmetric and positive definite matrices. Let $K_{\bar{p}} = [K_p \ K_{\dot{p}}]$ and

$$A_z = \begin{bmatrix} 0_3 & I_3 \\ 0_3 & 0_3 \end{bmatrix}, B_z = \begin{bmatrix} 0_3 \\ I_3 \end{bmatrix}.$$

Then the nominal position controller parameter matrix $K_{\bar{p}}$ can be given by $K_{\bar{p}} = \Pi_p^{-1}B_z^T Q_p$, where Q_p is the positive definite solution to the following Riccati equation as:

$$A_z^T Q_p + Q_p A_z + M_p - Q_p B_z \Pi_p^{-1} B_z^T Q_p = 0.$$

Considering the communication delays, one can obtain the new equivalent disturbance Δ_{pi}^* in the translational model, satisfying

$$\Delta_{pi}^*(t) = \Delta_{pi}(t) + \Delta_{hpj}(t) - \Delta_{hpj}(t-h), \quad (10)$$

where $\Delta_{hpj}(t) = \alpha_F \sum_{j \in N} a_{ij}K_p p_j(t) + \alpha_F \sum_{j \in N} a_{ij}K_{\dot{p}} \dot{p}_j(t)$, and $\Delta_{hpj}(t) - \Delta_{hpj}(t-h)$ represents the mismatched term caused by the communication delays. Based on a robust filter $F_{pi}(s)$, u_{pi}^R can be constructed as:

$$u_{pi}^R(s) = -F_{pi}(s)\Delta_{pi}^*(s), \quad i \in \Phi, \quad (11)$$

where $F_{pi}(s) = \text{diag}\{F_{p1,i}(s), F_{p2,i}(s), F_{p3,i}(s)\}$, $F_{pl,i}(s) = f_{pl,i}^2 / (s + f_{pl,i})^2$ ($l = 1, 2, 3$) with the positive robust filter parameters $f_{pl,i}$ to be selected, and $f_{pi} = \text{diag}\{f_{pl,i}\} \in \mathbb{R}^{3 \times 3}$. From [23], [24], one can see that larger robust filter parameters yield wider frequency bandwidths. In this case, $F_{pi}(s)$ can get closer to a unit matrix, and thus $u_{pi}^R(s)$ can get closer to the equivalent disturbance Δ_{pi}^* . However, Δ_{pi}^* cannot be measured directly in practical applications. Then, from (6), one has that

$$\Delta_{pi}^* = \ddot{p}_i - C_{p1i}^N \dot{p}_i - C_{p2i}^N p_i - u_{pi}. \quad (12)$$

Therefore, substituting (12) to (11), one can obtain the realization of $u_{pi}^R(t)$ by the following state-space form as:

$$\begin{aligned} \dot{z}_{1i}^p(t) &= -f_{pi}z_{1i}^p(t) + u_{pi}(t) \\ &\quad - (f_{pi}^2 + C_{p1i}^N f_{pi} - C_{p2i}^N) p_i(t), \\ \dot{z}_{2i}^p(t) &= -f_{pi}z_{2i}^p(t) + (2f_{pi} + C_{p1i}^N) p_i(t) + z_{1i}^p(t), \\ u_{pi}^R(t) &= -f_{pi}^2 p_i(t) + f_{pi}^2 z_{2i}^p(t), \quad i \in \Phi, \end{aligned} \quad (13)$$

where $z_{1i}^p(t), z_{2i}^p(t) \in \mathbb{R}^{3 \times 3}$ are the filter states.

Remark 2: It should be pointed out that h represents the communication delay when satellite i obtains information

from its neighbor. In fact, h is involved in the control input, which can affect the global closed-loop control system. It should be noted that there exists a communication delay h when satellite i receives information from its neighbors. The communication delays are nonnegative and assumed to be uniformly bounded functions, satisfying $\bar{h} = \max \|h\|_\infty < \infty$ and $\bar{h}_d = \max \|\dot{h}\|_\infty < 1$.

B. ROTATIONAL FORMATION CONTROLLER DESIGN

Similarly to the design process of the translational formation controller, the virtual rotational control input $u_{\sigma i}(t)$ can be divided into the following two parts:

$$u_{\sigma i}(t) = u_{\sigma i}^F(t) + u_{\sigma i}^R(t), \quad i \in \Phi, \quad (14)$$

where $u_{\sigma i}^F(t), u_{\sigma i}^R(t) \in \mathbb{R}^{3 \times 1}$ are the nominal control part and robust control part, respectively. The nominal control part $u_{\sigma i}^F(t)$ is designed similarly to $u_{p i}^F(t)$ as:

$$\begin{aligned} u_{\sigma i}^F = & -\eta_F \sum_{j \in N} a_{ij} K_\sigma (\sigma_i(t) - \sigma_j(t-h) - \zeta_{\sigma i}) \\ & - \eta_F \sum_{j \in N} a_{ij} K_{\dot{\sigma}} (\dot{\sigma}_i(t) - \dot{\sigma}_j(t-h) - \dot{\zeta}_{\sigma i}) \\ & - \eta_F \beta_{li} K_\sigma (\sigma_i(t) - \zeta_{\sigma i} - \sigma^r(t)) \\ & - \eta_F \beta_{li} K_{\dot{\sigma}} (\dot{\sigma}_i(t) - \dot{\zeta}_{\sigma i} - \dot{\sigma}^r(t)), \end{aligned} \quad (15)$$

where $K_\sigma, K_{\dot{\sigma}} \in \mathbb{R}^{3 \times 3}$ are diagonal nominal controller parameter matrices. Let $K_{\bar{\sigma}} = [K_\sigma \ K_{\dot{\sigma}}]$. Considering symmetric and positive definite matrices $M_\sigma = M_\sigma^T \in \mathbb{R}^{6 \times 6}$ and $\Pi_\sigma = \Pi_\sigma^T \in \mathbb{R}^{3 \times 3}$, one can obtain $K_{\bar{\sigma}}$ by $K_{\bar{\sigma}} = \Pi_\sigma^{-1} B_z^T Q_\sigma$, where Q_σ is the positive definite solution to the Riccati equation

$$A_z^T Q_\sigma + Q_\sigma A_z + M_\sigma - Q_\sigma B_z \Pi_\sigma^{-1} B_z^T Q_\sigma = 0.$$

By considering the communication delays, one can obtain the new equivalent disturbance $\Delta_{\sigma i}^*$ in the rotational model, satisfying

$$\Delta_{\sigma i}^*(t) = \Delta_{\sigma i}(t) + \Delta_{h\sigma j}(t) - \Delta_{h\sigma j}(t-h), \quad (16)$$

where $\Delta_{h\sigma j}(t) = \alpha_F \sum_{j \in N} a_{ij} K_\sigma \sigma_j(t) + \alpha_F \sum_{j \in N} a_{ij} K_{\dot{\sigma}} \dot{\sigma}_j(t)$, and $\Delta_{h\sigma j}(t) - \Delta_{h\sigma j}(t-h)$ indicates the mismatched term caused by the communication delays, which will affect communication between satellites and reduce the performance of the controller. Similarly, the robust part $u_{\sigma i}^R$ can be constructed as:

$$u_{\sigma i}^R(s) = -F_{\sigma i}(s) \Delta_{\sigma i}^*(s), \quad (17)$$

where $F_{\sigma i}(s) = \text{diag}\{F_{\sigma 1,i}(s), F_{\sigma 2,i}(s), F_{\sigma 3,i}(s)\}$ and $F_{\sigma l,i}(s) = f_{\sigma l,i}^2 / (s + f_{\sigma l,i})^2$ ($l = 1, 2, 3$) with the positive robust filter parameters $f_{\sigma l,i}$, and $f_{\sigma i} = \text{diag}\{f_{\sigma l,i}\} \in \mathbb{R}^{3 \times 3}$. $u_{\sigma i}^R(t)$ can be realized in a similar way as the following equations:

$$\begin{aligned} \dot{z}_{i1}^\sigma(t) &= -f_{\sigma 1} z_{i1}^\sigma(t) - f_{\sigma 1}^2 \sigma_i(t) + u_{\sigma i}(t), \\ \dot{z}_{i2}^\sigma(t) &= -f_{\sigma 2} z_{i2}^\sigma(t) + 2f_{\sigma 2} \sigma_i(t) + z_{i1}^\sigma(t), \\ u_{\sigma i}^R(t) &= -f_{\sigma 1}^2 \sigma_i(t) + f_{\sigma 1}^2 z_{i2}^\sigma(t), \quad i \in \Phi. \end{aligned} \quad (18)$$

Remark 3: A relative motion model including the leader satellite and the deputy satellites was discussed in [12], and the resulted formation controller was distributed based on the model. In the current paper, the proposed formation controllers expressed in (8), (9), (11), (14), (15), and (17) are distributed, because controller design only needs information from satellite i and its neighbors.

IV. ROBUSTNESS PROPERTIES

Define the translational and rotational tracking errors of satellite i as $e_{pi} = [e_{p i,i}] = p_i - \zeta_{pi} - p^r \in \mathbb{R}^{3 \times 1}$ and $e_{\sigma i} = [e_{\sigma j,i}] = \sigma_i - \zeta_{\sigma i} - \sigma^r \in \mathbb{R}^{3 \times 1}$. Let $X_{pi} = [e_{pi}^T \ \dot{e}_{pi}^T]^T = [X_{pj,i}] \in \mathbb{R}^{6 \times 1}$ and $X_{\sigma i} = [e_{\sigma i}^T \ \dot{e}_{\sigma i}^T]^T = [X_{\sigma j,i}] \in \mathbb{R}^{6 \times 1}$. Then, by combining (6), (8), (9), (14), and (15), one can obtain the error system model for satellite i as follows:

$$\begin{aligned} \dot{X}_{pi}(t) &= -\eta_F B_z \sum_{j \in N} a_{ij} K_p (e_{pi}(t) - e_{pj}(t)) \\ &\quad - \eta_F B_z \sum_{j \in N} a_{ij} K_{\dot{p}} (\dot{e}_{pi}(t) - \dot{e}_{pj}(t)) \\ &\quad - \eta_F \beta_{li} B_z (K_p e_{pi}(t) + K_{\dot{p}} \dot{e}_{pi}(t)) \\ &\quad + A_z X_{pi}(t) + B_z (u_{pi}^R(t) + \Delta_{pi}^*(t)), \\ \dot{X}_{\sigma i}(t) &= -\eta_F B_z \sum_{j \in N} a_{ij} K_\sigma (e_{\sigma i}(t) - e_{\sigma j}(t)) \\ &\quad - \eta_F B_z \sum_{j \in N} a_{ij} K_{\dot{\sigma}} (\dot{e}_{\sigma i}(t) - \dot{e}_{\sigma j}(t)) \\ &\quad - \eta_F \beta_{li} B_z (K_\sigma e_{\sigma i}(t) + K_{\dot{\sigma}} \dot{e}_{\sigma i}(t)) \\ &\quad + A_z X_{\sigma i}(t) + B_z (u_{\sigma i}^R(t) + \Delta_{\sigma i}^*(t)). \end{aligned} \quad (19)$$

Now, the global closed-loop error system can be rewritten as:

$$\begin{aligned} \dot{X}_p(t) &= (I_N \otimes B_z) (u_p^R(t) + \Delta_p^*(t)) \\ &\quad + (I_N \otimes A_z - \eta_F(L + B_L) \otimes B_z K_{\bar{p}}) X_p(t) \\ &= A_{\bar{p}} X_p(t) + B_z \tilde{\Delta}_p(t), \\ \dot{X}_\sigma(t) &= (I_N \otimes B_z) (u_\sigma^R(t) + \Delta_\sigma^*(t)) \\ &\quad + (I_N \otimes A_z - \eta_F(L + B_L) \otimes B_z K_{\bar{\sigma}}) X_\sigma(t) \\ &= A_{\bar{\sigma}} X_\sigma(t) + B_z \tilde{\Delta}_\sigma(t), \end{aligned} \quad (20)$$

where $B_L = \text{diag}\{\beta_{li}\} \in \mathbb{R}^N$, $X_p \in \mathbb{R}^{6N \times 1}$ and $X_\sigma \in \mathbb{R}^{6N \times 1}$. Let $\lambda_i(i \in \Phi)$ represent the eigenvalues of $(L + B_L)$ and $\lambda_{\min} = \min_{i \in \Phi} \text{Re}(\lambda_i)$. From Theorem 1 in [26], when the graph G has a spanning tree and the root can obtain the information from the virtual leader, if $\eta_F \geq \lambda_{\min}/2$, $A_{\bar{p}}$ and $A_{\bar{\sigma}}$ are asymptotically stable. Because the effectiveness of the nonlinear model for satellite has been validated by the experiments and our proposed robust formation control method has been checked by simulation tests based, our proposed robust formation control method can be suitable for

the multiple satellite s to achieve the real flying formations in experimental tests.

The robust compensating inputs $u_{pi}^R(t)$ in (11) and $u_{\sigma i}^R(t)$ in (17) can be represented by the following state-space forms:

$$\begin{aligned} \dot{X}_{Rkl,i}(t) &= A_{Rkl,i}(f_{kl,i})X_{Rkl,i}(t) + c_{2,1}\Delta_{kl,i}^*, \\ u_{kl,i}^R(t) &= -c_{2,2}^T f_{kl,i} X_{Rkl,i}(t), k = p, \sigma; l = 1, 2, 3, \end{aligned} \quad (21)$$

where

$$A_{Rkl,i}(f_{kl,i}) = \begin{bmatrix} -f_{kl,i} & 0 \\ f_{kl,i} & -f_{kl,i} \end{bmatrix}.$$

Let $X_{Rp}(t) = [X_{Rp1,i}^T(t), X_{Rp2,i}^T(t), X_{Rp3,i}^T(t)]^T \in \mathbb{R}^{N \times 1}$, $X_{R\sigma}(t) = [X_{R\sigma1,i}^T(t), X_{R\sigma2,i}^T(t), X_{R\sigma3,i}^T(t)]^T \in \mathbb{R}^{N \times 1}$, $\hat{X}_k(t) = [X_k^T(t), X_{Rk}^T(t)]^T (k = p, \sigma)$, $A_\Delta = \text{diag}\{-c_{2,2}^T f_{kl,i}\} \in \mathbb{R}^{3N \times 6N}$, $A_R = \text{diag}\{A_{Rkl,i}(f_{kl,i})\} \in \mathbb{R}^{6N \times 6N}$, $B_{\Delta 2} = \text{diag}\{c_{2,1}\} \in \mathbb{R}^{6N \times 3N} (l = 1, 2, 3)$, $B_{\Delta 1} = B_{k\Delta}$, and $\Delta_k^*(t) = [\Delta_{ki}^*(t)] \in \mathbb{R}^{N \times 1}$. From (20) and (21), the translational and rotational error models can be rewritten as:

$$\dot{\hat{X}}_k(t) = \hat{A}_k \hat{X}_k(t) + \hat{B}_k \Delta_k^*(t), k = p, \sigma, \quad (22)$$

where

$$\hat{A}_k = \begin{bmatrix} A_{\bar{k}} & B_{\bar{z}} A_\Delta \\ 0_{6N \times 6N} & A_R \end{bmatrix}, \hat{B}_k = \begin{bmatrix} B_{\Delta 1} \\ B_{\Delta 2} \end{bmatrix}.$$

The equivalent disturbances involved communication delays Δ_p^* and Δ_σ^* are assumed to satisfy

$$\begin{aligned} \|\Delta_k^*(t)\| &\leq \sum_{l=0}^1 \lambda_{ekl} \|E(t - h_l(t))\| + \sum_{l=0}^1 \lambda_{ukl} \|u_k(t - h_l(t))\| \\ &\quad + \gamma_{kd}, k = p, \sigma; l = 0, 1, \end{aligned}$$

where λ_{ekl} and λ_{ukl} are positive constants, γ_{kd} is uniformly bounded positive function involving the external disturbance d_k , and $E(t) = [e_p^T(t), \dot{e}_p^T(t), e_\sigma^T(t), \dot{e}_\sigma^T(t)]^T$. From (4) and (8), the equivalent disturbances Δ_p^* and Δ_σ^* satisfy that

$$\begin{aligned} \|\Delta_k^*(t)\| &\leq \sum_{l=0}^1 \lambda_{ekl} \|E(t - h_l(t))\| + \gamma_{kd} \\ &\quad + \sum_{l=0}^1 \lambda_{ukl} (\lambda_{kE} \|E(t - h_l(t))\|) \\ &\quad + \sum_{l=0}^1 \lambda_{ukl} (f_{km} \|X_{Rk}(t - h_l(t))\|), \end{aligned} \quad (23)$$

where $\lambda_{kE} (k = p, \sigma)$ are positive constants, $X_{Rk}(t) = \text{diag}(X_{Rk1}(t), X_{Rk2}(t), X_{Rk3}(t))$, $f_{km} = \|f_{ki}\|$, $\bar{h}_e = \max_l \|h_l\|_\infty$, $\bar{h}_{de} = \max_l \|\dot{h}_l\|_\infty$, and $h_0(t) = 0$. Define $\kappa = \|\Pi_p^{-1} B_z^T\|$, λ_{uk0} and λ_{uk1} are positive constants and selected to satisfy $2\kappa \lambda_{uk1} < [1 - \kappa(3\lambda_{uk0} + \lambda_{uk1})](1 - \bar{h}_e)$. The delay \bar{h}_e cannot be arbitrarily increased. Denote $P_k (k = p, \sigma)$ as the

solution to the Lyapunov equation: $P_k \hat{A}_k + \hat{A}_k^T P_k = -I_{12N}$. From (12), one can obtain that the matrix A_k is Hurwitz, thereby P_k is positive definite. There exists a positive constant λ_{Bk} satisfy

$$\|P_k \hat{B}_k\| \leq \lambda_{Bk} f_{km}^{-1}, k = p, \sigma.$$

Theorem 1: Consider the translational and rotational model of the satellite in (1) and (4), and the robust formation controller proposed in Section III. For a given initial time t_0 , a given bounded and piecewise continuous initial state $E(\tau)$, $\tau \in [t_0 - \bar{h}_e, t_0]$, and a positive constant ε , there exist positive constants $k_i (k = p, \sigma)$ and T such that for any f , $E_k(t)$ is uniformly bounded for $t \geq t_0$ and satisfies that $\|E(t)\| \leq \varepsilon$, $\forall t \geq \underline{T}$.

Proof: Consider the Lyapunov function candidate without the communication delays as:

$$V_1(\hat{X}(t)) = \sum_{k=p,\sigma} \hat{X}_k^T(t) P_k \hat{X}_k(t). \quad (24)$$

One can yield its derivative as follows:

$$\begin{aligned} \dot{V}_1(\hat{X}(t)) &= - \sum_{k=p,\sigma} (\|E_k(t)\|^2 + \|X_{Rk}(t)\|^2) \\ &\quad + \sum_{k=p,\sigma} 2\hat{X}_k^T(t) P_k \hat{B}_k \Delta_k(t) \\ &\leq - \sum_{k=p,\sigma} (\|E_k(t)\|^2 + \|X_{Rk}(t)\|^2) \\ &\quad + \sum_{k=p,\sigma} 2(\|E_k(t)\| + \|X_{Rk}(t)\|) \lambda_{Bk} f_{km}^{-1} \|\Delta_k^*(t)\|. \end{aligned} \quad (25)$$

Define $\xi_{ek} = \sum_{l=0}^1 \lambda_{Bk} \lambda_{ukl}$, $\xi_{efk} = \sum_{l=0}^1 \lambda_{Bk} \lambda_{ekl} + \sum_{l=0}^1 \lambda_{Bk} \lambda_{ukl} \lambda_{kE}$, $\xi_{uk} = \sum_{l=0}^1 \lambda_{Bk} \lambda_{ukl}$, $\xi_{ufk} = \sum_{l=0}^1 \lambda_{Bk} \lambda_{ekl} + \sum_{l=0}^1 \lambda_{Bk} \lambda_{ukl} \lambda_{kE}$, $\xi_{esfk} = 2 \sum_{l=0}^1 \lambda_{Bk} \lambda_{ekl}$, $\xi_{usk} = 2 \sum_{l=0}^1 \lambda_{Bk} \lambda_{ekl}$, and $\xi_{\gamma k} = 2 \lambda_{Bk} \gamma_{kd}$. Substituting (23) into (25), one can obtain that

$$\begin{aligned} \dot{V}_1(\hat{X}(t)) &\leq - \sum_{k=p,\sigma} (1 - \xi_{ek} - \xi_{efk} f_{km}^{-1}) \|E_k(t)\|^2 \\ &\quad - \sum_{k=p,\sigma} (1 - \xi_{uk} - \xi_{ufk} f_{km}^{-1}) \|X_{Rk}(t)\|^2 \\ &\quad + \sum_{k=p,\sigma} \xi_{esfk} \|E_k(t - h_l(t))\|^2 f_{km}^{-1} \\ &\quad + \sum_{k=p,\sigma} \xi_{usk} \|X_{Rk}(t - h_l(t))\|^2 \\ &\quad + \sum_{k=p,\sigma} \xi_{\gamma k} \|E_k(t)\| f_{km}^{-1} \\ &\quad + \sum_{k=p,\sigma} \xi_{\gamma k} \|X_{Rk}(t)\| f_{km}^{-1}. \end{aligned} \quad (26)$$

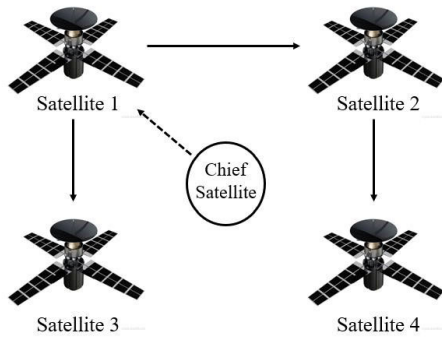


FIGURE 1. Communication graph of satellites.

Then, the communication delays are introduced to obtain the final Lyapunov function candidate as:

$$\begin{aligned}
 V(\hat{X}(t), t) &= V_1(\hat{X}(t)) \\
 &+ \sum_{k=p,\sigma} \sum_{l=0}^1 \xi_{NR} \int_{t-h_l(t)}^t \|X_{Rk}(\tau)\|^2 d\tau \\
 &+ \sum_{k=p,\sigma} \sum_{l=0}^1 \xi_{NE} \int_{t-h_l(t)}^t \|E_k(\tau)\|^2 d\tau, \quad (27)
 \end{aligned}$$

where ξ_{NE} and ξ_{NR} are positive constants, and satisfy $1 - 2\xi_{NE} > \xi_{ek}$, $1 - 2\xi_{NR} > \xi_{uk}$, and $2(1 - \bar{h}_{de})\xi_{NR} > \xi_{usk}$. By differentiating (27), one can obtain that

$$\begin{aligned}
 \dot{V}(\hat{X}(t), t) &\leq \dot{V}_1(\hat{X}(t)) + \sum_{k=p,\sigma} \sum_{l=0}^1 \xi_{NE} \|E_k(t)\|^2 \\
 &- \sum_{k=p,\sigma} \sum_{l=0}^1 \xi_{NE} (1 - \bar{h}_{de}) \|E_k(t - h_l(t))\|^2 \\
 &+ \sum_{k=p,\sigma} \sum_{l=0}^1 \xi_{NR} \|X_{Rk}(t)\|^2 \\
 &- \sum_{k=p,\sigma} \sum_{l=0}^1 \xi_{NR} (1 - \bar{h}_{de}) \|X_{Rk}(t - h_l(t))\|^2. \quad (28)
 \end{aligned}$$

Let $\pi_{ek} = 1 - 2\xi_{NE} - \xi_{ek} - \xi_{efk}f_{km}^{-1}$, $\pi_{Rk} = 1 - 2\xi_{NR} - \xi_{uk} - \xi_{ufk}f_{km}^{-1}$, $\pi_{esk} = 2(1 - \bar{h}_{de})\xi_{NE} - \xi_{esfk}f_{km}^{-1}$, $\pi_{Rsk} = 2(1 - \bar{h}_{de})\xi_{NR} - \xi_{usk}$, and $\pi_{\gamma k} = \xi_{\gamma k}f_{km}^{-1}$. Substituting (26) into (28), one can obtain that:

$$\begin{aligned}
 \dot{V}(\hat{X}(t), t) &\leq - \sum_{k=p,\sigma} \pi_{ek} \|E_k(t)\|^2 - \sum_{k=p,\sigma} \pi_{Rk} \|X_{Rk}(t)\|^2 \\
 &- \sum_{k=p,\sigma} \pi_{Rsk} \|X_{Rk}(t - h_d(t))\|^2 \\
 &- \sum_{k=p,\sigma} \pi_{esk} \|E_k(t - h_d(t))\|^2 \\
 &+ \sum_{k=p,\sigma} \pi_{\gamma k} \|E_k(t)\| + \sum_{k=p,\sigma} \pi_{\gamma k} \|X_{Rk}(t)\|. \quad (29)
 \end{aligned}$$

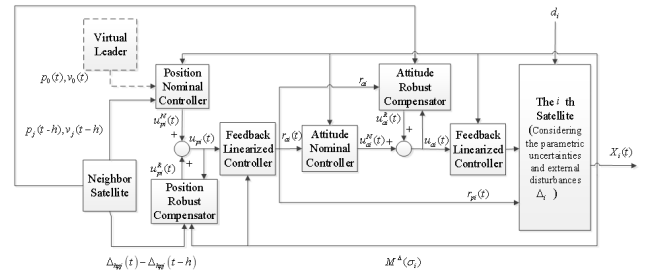


FIGURE 2. Structure of the proposed controller.

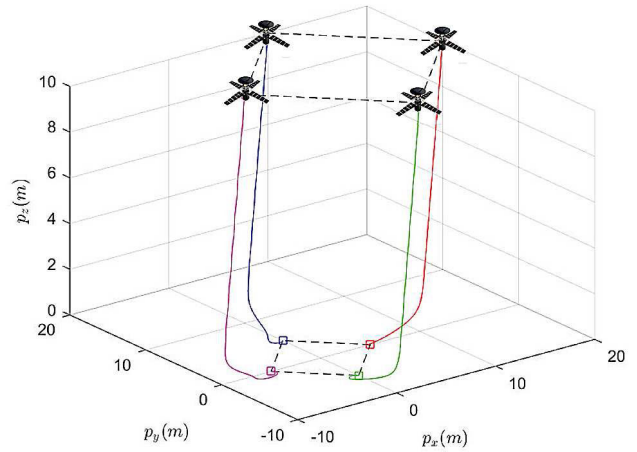


FIGURE 3. Three-dimensional trajectory by the proposed controller.

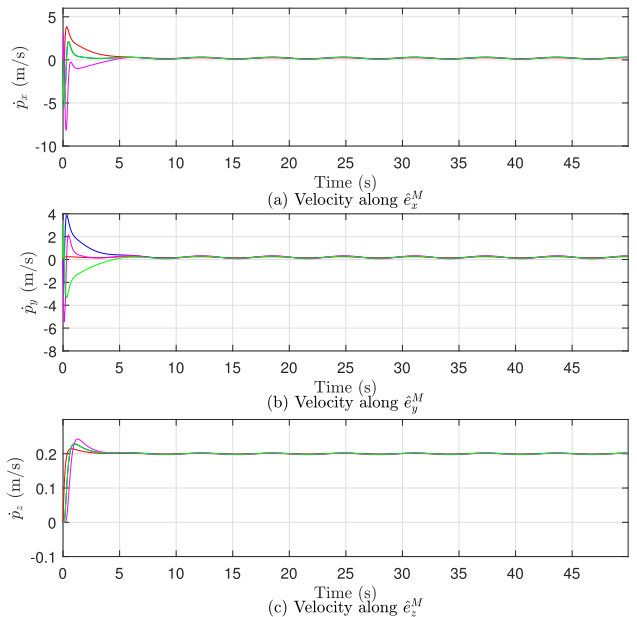


FIGURE 4. Velocity response by the proposed controller.

One can observe that if the robust filter parameters f_{km} ($k = p, \sigma$) satisfy

$$\begin{aligned}
 f_{km} &> \xi_{efk} / (1 - 2\xi_{NE} - \xi_{ek}), \\
 f_{km} &> \xi_{ufk} / (1 - 2\xi_{NR} - \xi_{uk}), \\
 f_{km} &> \xi_{esfk} / 2(1 - \bar{h}_{de})\xi_{NE}, \quad k = p, \sigma,
 \end{aligned}$$

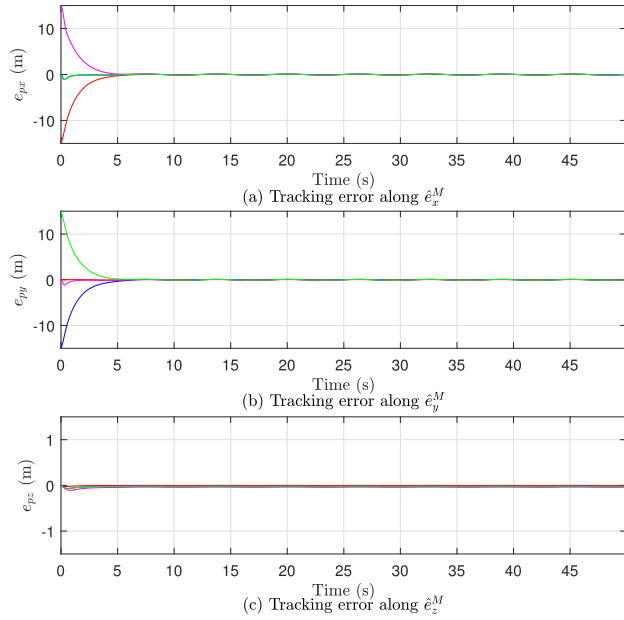


FIGURE 5. Translational tracking error by the proposed controller.

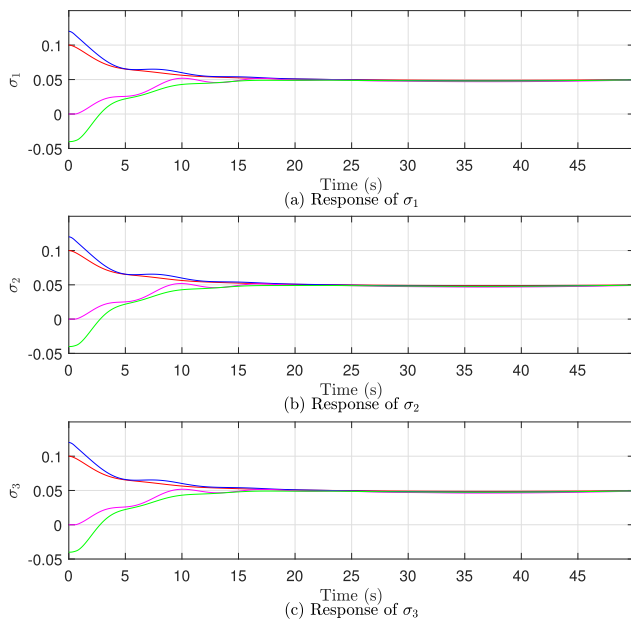


FIGURE 6. Rotational response by the proposed controller.

then, π_{ek} and π_{Rk} are positive, while π_{Rsk} , π_{esk} , and $\pi_{\gamma k}$ are nonnegative. Therefore, for a given initial time t_0 , a given bounded and piecewise continuous initial state $E(\tau)$, $\tau \in [t_0 - \bar{h}_e, t_0]$, and a positive constant ε , there exist positive constants f_{ki} ($k = p, \sigma$) and \underline{T} such that for any $f_{ki} > \underline{f}_{ki}$, $E_k(t)$ is uniformly bounded for $t \geq t_0$ and satisfies that $\|E(t)\| \leq \varepsilon, \forall t \geq \underline{T}$. \square

V. SIMULATION RESULTS

In this section, numerical simulation results of four satellites have been given to verify the effectiveness and advantages of

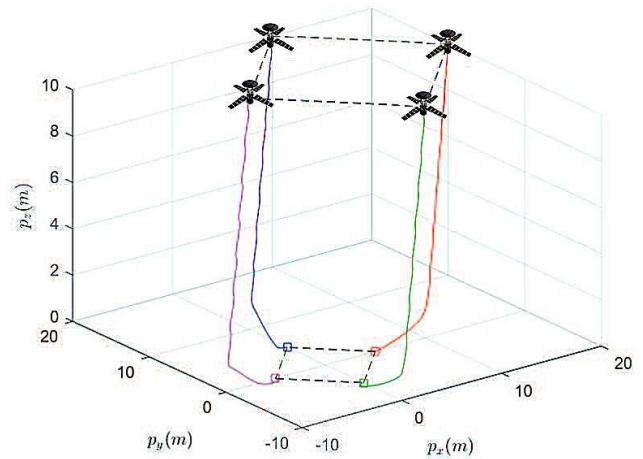


FIGURE 7. Three-dimensional trajectory by the leader-following controller.

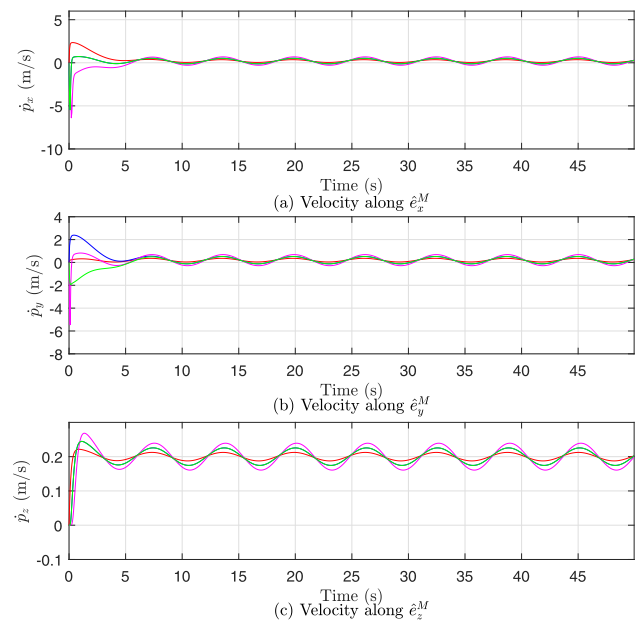


FIGURE 8. Velocity response by the leader-following controller.

the proposed formation controller, and thus $\Phi = \{1, 2, 3, 4\}$. The satellite model in Section II is used in the simulation test with the Earth's gravitational constant $\mu_g = 3.986 \times 10^{14}$, the nominal inertia matrix of each satellite $J_i^N = \text{diag}\{4.34, 4.33, 3.66\}$, and the leader satellite's orbit radius $r_{0L} = 7.4 \times 10^6$, and all parameters are in international units. The trajectory of the virtual leader is given by $p^r = [0.2t \ 0.2t \ 0.2t]^T$ and the desired attitude is $\sigma^r = [0.05 \ 0.05 \ 0.05]^T$. The four satellites are required to form a pentagon formation pattern as $\zeta_1 = 10(1 - e^{-t})c_{3,1}$, $\zeta_2 = 10(1 - e^{-t})c_{3,2}$, $\zeta_3 = -10(1 - e^{-t})c_{3,1}$, and $\zeta_4 = -10(1 - e^{-t})c_{3,2}$. Only satellite 1 can obtain the information from the virtual leader, and thereby $\beta_{11} = 1$, $\beta_{12} = 0$, $\beta_{13} = 0$, and $\beta_{14} = 0$. The topological relationship of the four satellites is described as Fig. 1 and structure of the proposed

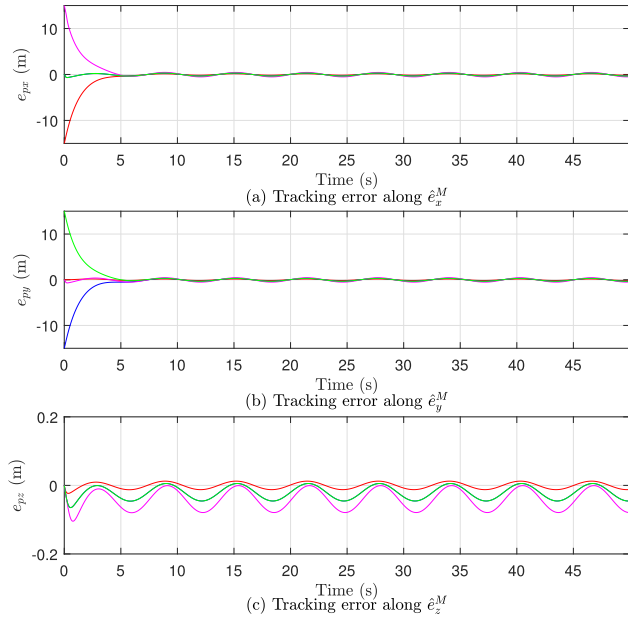


FIGURE 9. Translational tracking error by the leader-following controller.

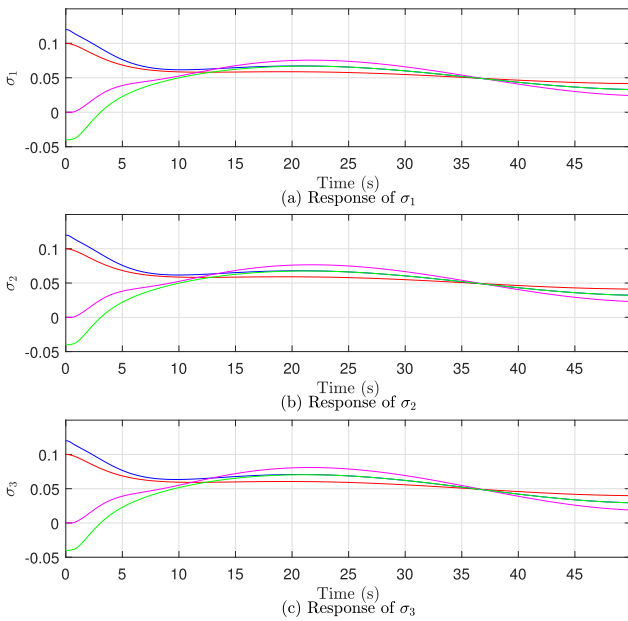


FIGURE 10. Rotational response by the leader-following controller.

controller is described as Fig. 2. The adjacency matrix A is given by

$$[A_{ij}] = \begin{bmatrix} 0 & 0 & 0 & 0 \\ 1 & 0 & 0 & 0 \\ 0 & 1 & 0 & 0 \\ 1 & 0 & 0 & 0 \end{bmatrix}.$$

The initial conditions of the four satellites are given as: $p_1(0) = [5 \ 0 \ 0]^T$, $p_2(0) = [0 \ 5 \ 0]^T$, $p_3(0) = [-5 \ 0 \ 0]^T$, $p_4(0) = [0 \ -5 \ 0]^T$, $\dot{p}_i(0) = [0 \ 0 \ 0]^T$ ($i \in \Phi$), $\sigma_1(0) = [0.1 \ 0.1 \ 0.1]^T$, $\sigma_2(0) = [0.12 \ 0.12 \ 0.12]^T$,

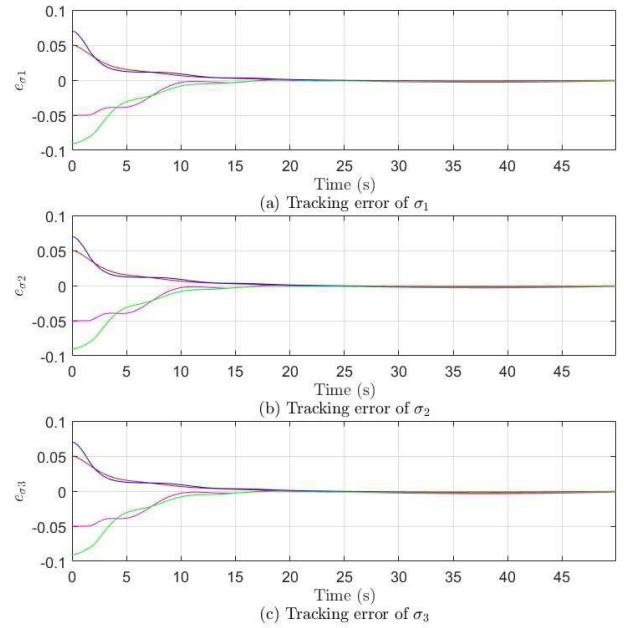


FIGURE 11. Rotational tracking error of four satellites with 0.3 s communication delay.

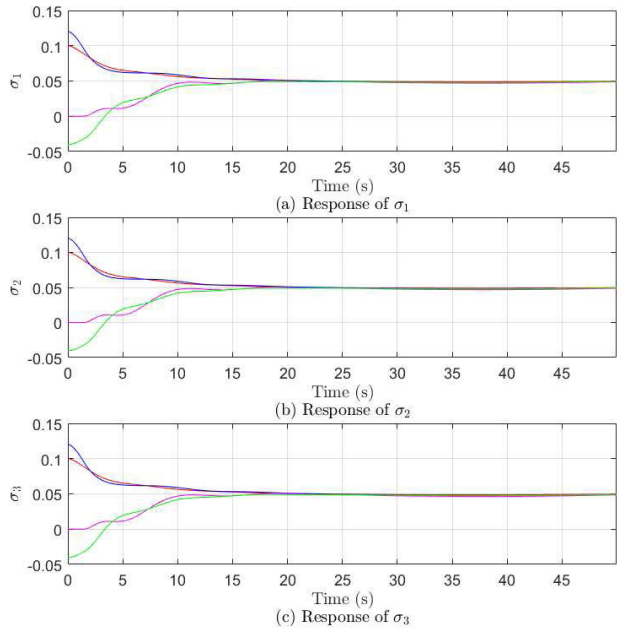


FIGURE 12. Rotational response of four satellites with 0.3 s communication delay.

$\sigma_3(0) = [0 \ 0 \ 0]^T$, and $\sigma_4(0) = [-0.04 \ -0.04 \ -0.04]^T$. The external disturbances used in [12] were time-invariant. However, in the current paper, time-varying and non-vanished disturbances are considered to simulate complex space environment. The real satellite parameters are chosen to be 15% larger than the nominal parameters and the external disturbance torques are selected as: $d_p = [5 \sin t \ 5 \sin t \ 0.1 \ sin t]^T$ for the position control input and $d_\tau = 0.3[\sin 0.5t \ \sin 0.5t \ \sin 0.5t]^T$ for the attitude torque.

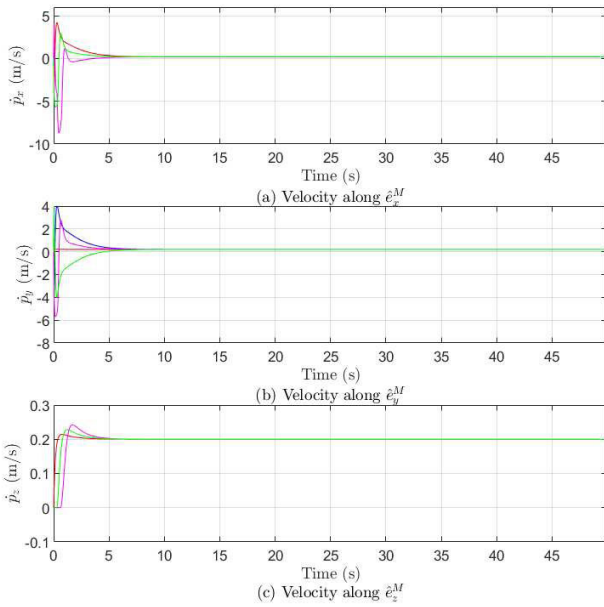


FIGURE 13. Velocity response of four satellites with 0.3 s communication delay.

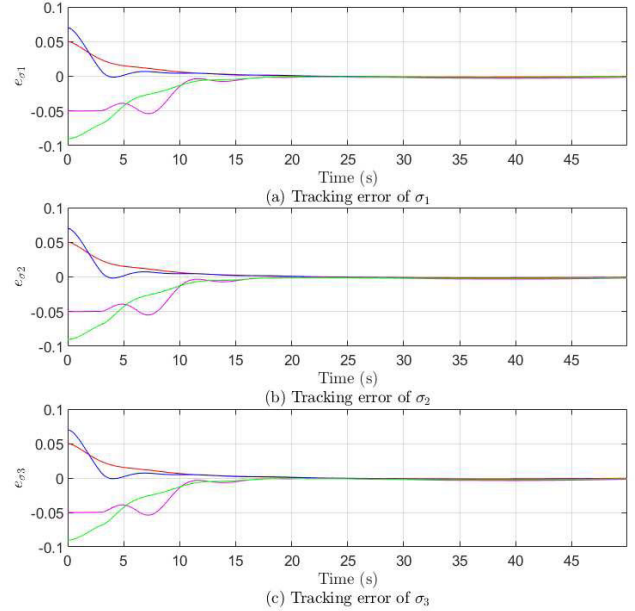


FIGURE 15. Rotational tracking error of four satellites with 0.6 s communication delay.

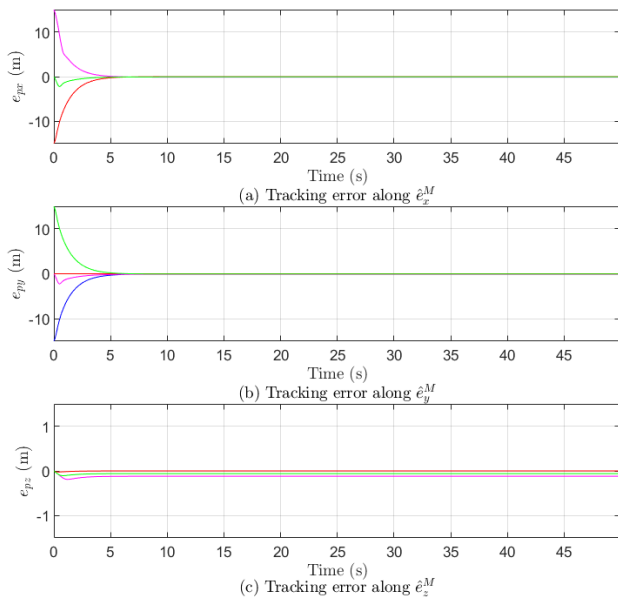


FIGURE 14. Translational tracking error of four satellites with 0.3s communication delay.

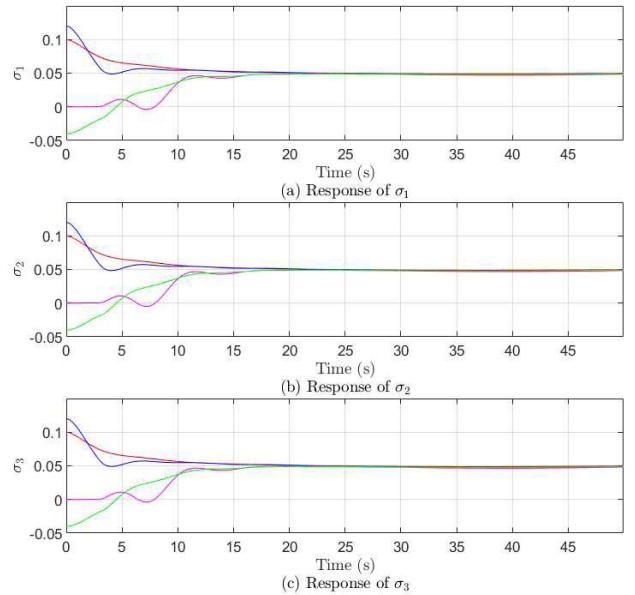


FIGURE 16. Rotational response of four satellites with 0.6 s communication delay.

The scalar coupling gain is set to be $\alpha_F = 1$. The communication delays are assumed that $\|h_e(t)\|_\infty \leq 0.1$ s. The nominal controller parameters are selected as: $K_p = \text{diag}\{20, 20, 5\}$, $K_{\dot{p}} = \text{diag}\{25, 25, 7\}$, $K_\sigma = \text{diag}\{100, 100, 100\}$, and $K_{\dot{\sigma}} = \text{diag}\{90, 90, 90\}$. The robust filter parameters are selected as $f_{p_i} = \text{diag}\{7, 7, 30\}$ and $f_{\sigma_i} = \text{diag}\{7, 7, 7\}$ according to Remark 4 for better control performance.

Figs. 3, 4, 5, and 6 depict the three-dimensional trajectory p_i , velocity response \dot{p}_i , translational tracking error e_{p_i} , and rotational response σ_i of the four satellites, respectively. The red, blue, pink, and black solid lines indicate Satellites 1-4,

and the black dotted line represents the formation pattern. It can be seen that the steady-state translational and rotational tracking errors are nearly 0.2 m and 0.003. Besides, the proposed robust formation controller in Section 3 is compared to a leader-following controller introduced in [27] for the satellite group. Limited types of uncertainties were discussed in stability analysis of the constructed global closed-loop control systems, the effects of the communication delays between neighboring satellites were ignored in the stability analysis of the [27]. The experimental result is a proof of theory. In addition to the above reasons, [27] depict the rotational response

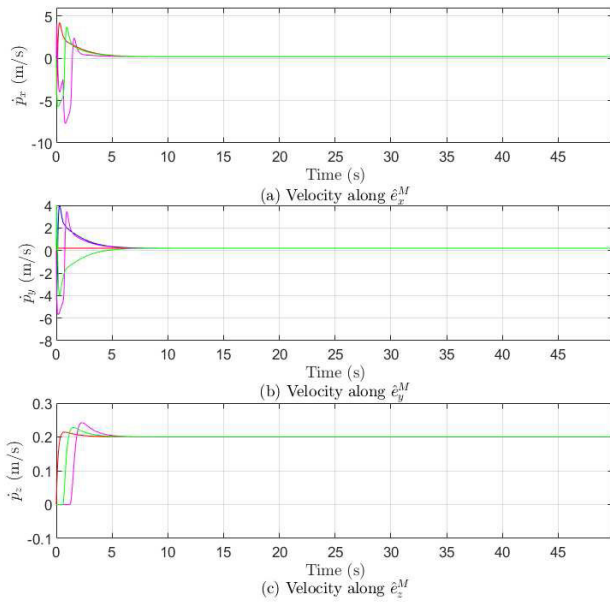


FIGURE 17. Velocity response of four satellites with 0.6 s communication delay.

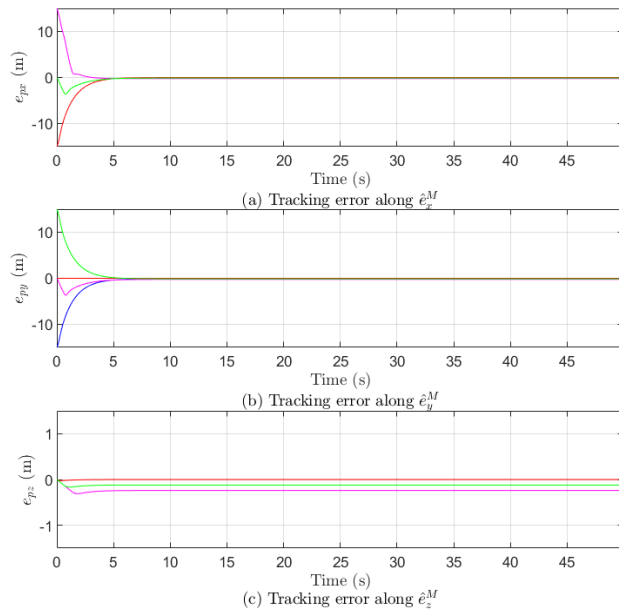


FIGURE 18. Translational tracking error of four satellites with 0.6 s communication delay.

of the four satellites by the proposed controller. Since the error of following two followers is independent of each other, the algorithm error is easy to diverge without feedback and compensation, which cannot affect the proposed controller. Figs. 7, 8, 9 and 10 show the formation trajectory, velocity response, translational tracking error and rotational response of the satellite group respectively, and the steady-state translational and rotational tracking errors are approximately 0.5 m and 0.03, by the leader-following formation control scheme. In Fig.6 and Fig.10, three rotational responses are close but different, the initial condition and the trace condition are close

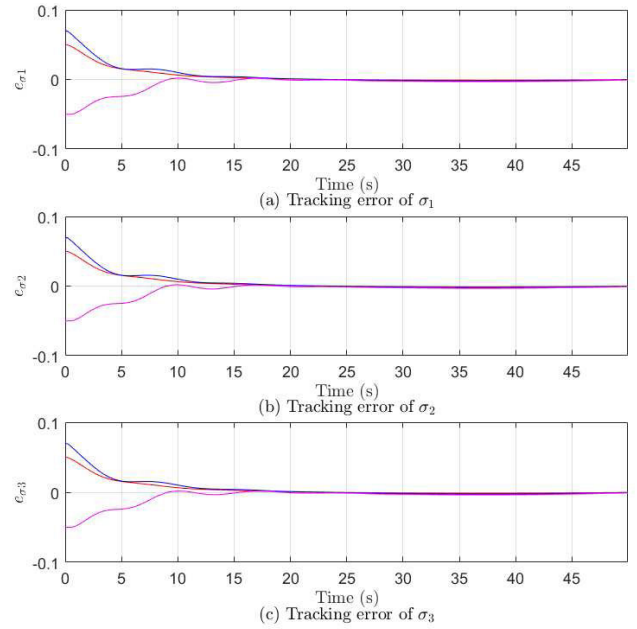


FIGURE 19. Rotational tracking error of three satellites with 0.1 s communication delay.

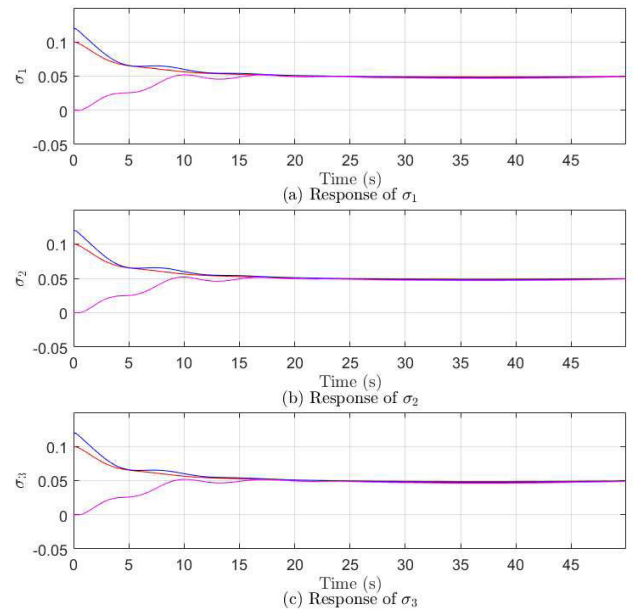


FIGURE 20. Rotational response of three satellites with 0.1 s communication delay.

to each other. But they will be slightly different caused by disturbance and uncertainty.

To test the effects of the delay, three sets of different time delays, i.e., $h=0.1$ s, $h=0.3$ s, $h=0.6$ s are set up respectively. At the same time, a different group is set up to test the effects of the number of satellites for the response comparison, with three satellites. Figs. 11, 12, 13 and 14 show the rotational tracking error e_{σ_i} , rotational response σ_i , velocity response \dot{p}_i , and translational tracking error e_{p_i} of four satellites with a communication delay of 0.3 s.

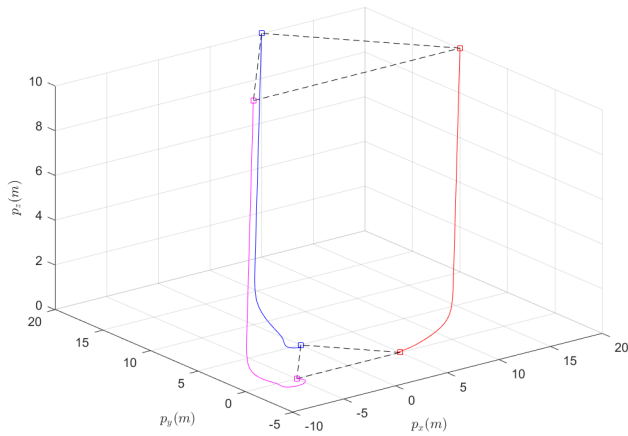


FIGURE 21. Three-dimensional trajectory of three satellites with 0.1 s communication delay.

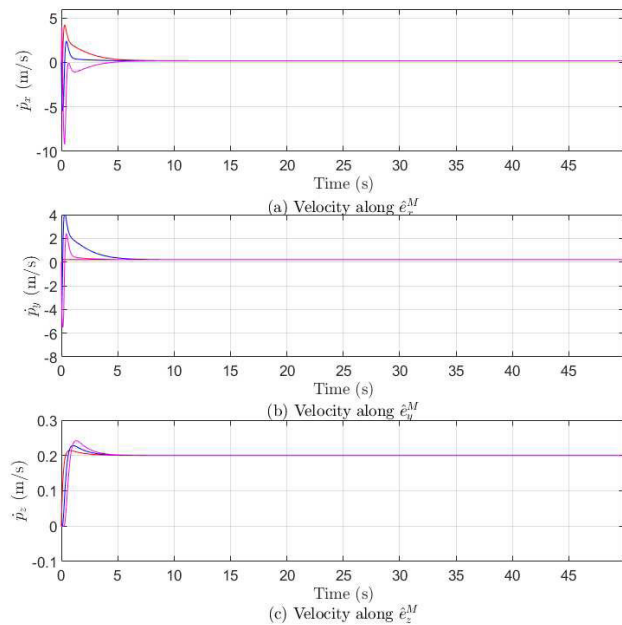


FIGURE 22. Velocity response of three satellites with 0.1 s communication delay.

Figs. 15, 16, 17 and 18 show the rotational tracking error e_{σ_i} , rotational response σ_i , velocity response \dot{p}_i , and translational tracking error e_{p_i} of four satellites with a communication delay of 0.6 s. Figs. 19, 20, 21, 23 and 23 show the rotational tracking error e_{σ_i} , rotational response σ_i , three-dimensional trajectory, velocity response \dot{p}_i , and translational tracking error e_{p_i} of three satellites with a communication delay of 0.1 s. It can be seen that the mutual influence between the satellites, the degree of curve fluctuation and the convergence time increase as the communication delay increases. And the impact decreases as the number of satellites decreases.

From these simulation results, one can observe that the desired translational and rotational tracking control can be better achieved under the influence of nonlinear dynamics, parametric uncertainties, external disturbances, and communication delays.

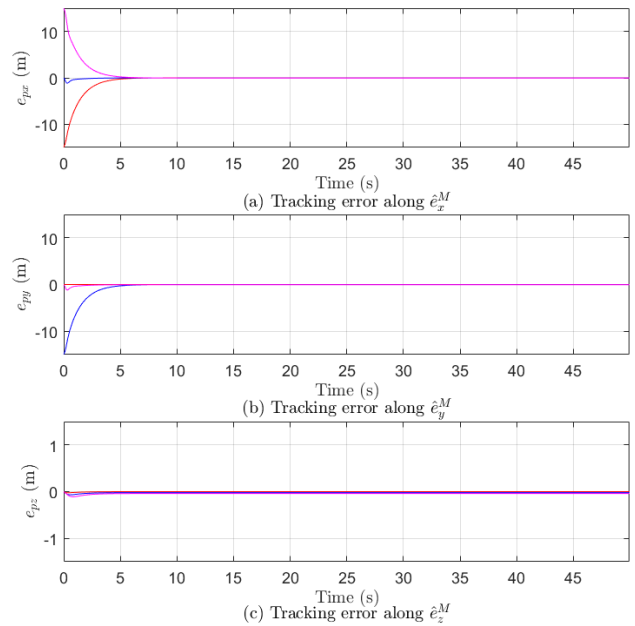


FIGURE 23. Translational tracking error of three satellites with 0.1 s communication delay.

VI. CONCLUSION

A robust formation controller design method is proposed to address the problem of satellite formation flying subject to nonlinear dynamics, parametric uncertainties, external disturbances, and communication delays. The proposed formation controller includes a translational controller and a rotational controller, to govern the translational motion and the rotational motion respectively. It is proven that the translational and rotational tracking errors of the global closed-loop control system can converge into a given neighborhood of the origin in a finite time. The numerical simulation results are given to demonstrate the effectiveness and advantages of the designed formation flying controller. The proposed method is applicable to almost all other flying agents, not just satellites. In future, the robust optimal controller via the reinforcement learning method will be studied to achieve the desired satellite formation flying. The new formation controller will be designed, independently of satellite model parameters.

REFERENCES

- [1] C. Wei, S.-Y. Park, and C. Park, "Optimal H_∞ robust output feedback control for satellite formation in arbitrary elliptical reference orbits," *Adv. Space Res.*, vol. 54, no. 6, pp. 969–989, Sep. 2014.
- [2] H. Zhang and P. Gurfil, "Cooperative orbital control of multiple satellites via consensus," *IEEE Trans. Aerosp. Electron. Syst.*, vol. 54, no. 5, pp. 2171–2188, Oct. 2018.
- [3] H.-S. Ahn, K. L. Moore, and Y. Chen, "Trajectory-keeping in satellite formation flying via robust periodic learning control," *Int. J. Robust Non-linear Control*, vol. 20, no. 14, pp. 1655–1666, Aug. 2010.
- [4] S.-H. Mok, Y.-H. Choi, and H.-C. Bang, "Collision avoidance using linear quadratic control in satellite formation flying," *Int. J. Aeronaut. Space Sci.*, vol. 11, no. 4, pp. 351–359, Dec. 2010.
- [5] L. Cao, Y. Chen, Z. Zhang, H. Li, and A. K. Misra, "Predictive smooth variable structure filter for attitude synchronization estimation during satellite formation flying," *IEEE Trans. Aerosp. Electron. Syst.*, vol. 53, no. 3, pp. 1375–1383, Jun. 2017.

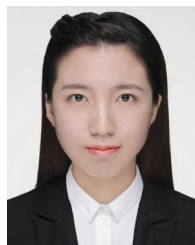
- [6] Y.-H. Lim and H.-S. Ahn, "Relative position keeping in satellite formation flying with input saturation," *J. Franklin Inst.*, vol. 351, no. 2, pp. 1112–1129, Feb. 2014.
- [7] M. A. A. Hallaj and N. Assadian, "Sliding mode control of electromagnetic tethered satellite formation," *Adv. Space Res.*, vol. 58, no. 4, pp. 619–634, Aug. 2016.
- [8] J. Xi, C. Wang, H. Liu, and Z. Wang, "Dynamic output feedback guaranteed-cost synchronization for multiagent networks with given cost budgets," *IEEE Access*, vol. 6, pp. 28923–28935, 2018.
- [9] P. Massioni, T. Keviczky, E. Gill, and M. Verhaegen, "A decomposition-based approach to linear time-periodic distributed control of satellite formations," *IEEE Trans. Control Syst. Technol.*, vol. 19, no. 3, pp. 481–492, May 2011.
- [10] Z. Hu and J. Yang, "Distributed optimal formation algorithm for multi-satellites system with time-varying performance function," *Int. J. Control*, vol. 93, no. 5, pp. 1015–1026, Jun. 2018.
- [11] W. Ren, "Distributed cooperative attitude synchronization and tracking for multiple rigid bodies," *IEEE Trans. Control Syst. Technol.*, vol. 18, no. 2, pp. 383–392, Mar. 2010.
- [12] H. Min, Z. Gao, F. Sun, Y. Wang, and S. Wang, "Distributed six degree-of-freedom spacecraft formation control with possible switching topology," *IET Control Theory Appl.*, vol. 5, no. 9, pp. 1120–1130, Jun. 2011.
- [13] Y. Huang and Y. Jia, "Distributed finite-time output feedback synchronisation control for six DOF spacecraft formation subject to input saturation," *IET Control Theory Appl.*, vol. 12, no. 4, pp. 532–542, Mar. 2018.
- [14] H. Liu, Y. Tian, F. L. Lewis, Y. Wan, and K. P. Valavanis, "Robust formation flying control for a team of satellites subject to nonlinearities and uncertainties," *Aerosp. Sci. Technol.*, vol. 95, pp. 1–9, Dec. 2019.
- [15] H. Liu, Y. Tian, and F. L. Lewis, "Robust trajectory tracking in satellite time-varying formation flying," *IEEE Trans. Cybern.*, early access, Jan. 9, 2020, doi: [10.1109/TCYB.2019.2960363](https://doi.org/10.1109/TCYB.2019.2960363).
- [16] R. Liu, X. Cao, and M. Liu, "Finite-time synchronization control of spacecraft formation with network-induced communication delay," *IEEE Access*, vol. 5, pp. 27242–27253, 2017.
- [17] Q. Hu, J. Zhang, and G. Ma, "L2-gain based adaptive sliding mode coordinated attitude control of satellite formation with time-varying delays," *Syst. Eng. Electron.*, vol. 35, no. 11, pp. 2356–2363, Nov. 2013.
- [18] J. Erdong and S. Zhaowei, "Robust attitude synchronisation controllers design for spacecraft formation," *IET Control Theory Appl.*, vol. 3, no. 3, pp. 325–339, Mar. 2009.
- [19] Q. Wang, Z. Duan, and Y. Lv, "Distributed attitude synchronization control for multiple flexible spacecraft without modal variable measurement," *Int. J. Robust Nonlinear Control*, vol. 28, no. 10, pp. 3435–3453, Mar. 2018.
- [20] I. Chang, S.-Y. Park, and K.-H. Choi, "Decentralized coordinated attitude control for satellite formation flying via the state-dependent Riccati equation technique," *Int. J. Non-Linear Mech.*, vol. 44, no. 8, pp. 891–904, Oct. 2009.
- [21] W. Deng, J. Yao, and D. Ma, "Time-varying input delay compensation for nonlinear systems with additive disturbance: An output feedback approach," *Int. J. Robust Nonlinear Control*, vol. 28, no. 1, pp. 31–52, May 2017.
- [22] W. Deng and J. Yao, "Extended-state-observer-based adaptive control of electrohydraulic servomechanisms without velocity measurement," *IEEE/ASME Trans. Mechatronics*, vol. 25, no. 3, pp. 1151–1161, Jun. 2020.
- [23] H. Liu, X. Wang, and Y. Zhong, "Quaternion-based robust attitude control for uncertain robotic quadrotors," *IEEE Trans. Ind. Informat.*, vol. 11, no. 2, pp. 406–415, Apr. 2015.
- [24] H. Liu, T. Ma, F. L. Lewis, and Y. Wan, "Robust formation control for multiple quadrotors with nonlinearities and disturbances," *IEEE Trans. Cybern.*, vol. 50, no. 4, pp. 1362–1371, Apr. 2020.
- [25] H. Liu, G. Lu, and Y. Zhong, "Robust LQR attitude control of a 3-DOF laboratory helicopter for aggressive maneuvers," *IEEE Trans. Ind. Electron.*, vol. 60, no. 10, pp. 4627–4636, Oct. 2013.
- [26] H. Zhang, F. L. Lewis, and A. Das, "Optimal design for synchronization of cooperative systems: State feedback, observer and output feedback," *IEEE Trans. Autom. Control*, vol. 56, no. 8, pp. 1948–1952, Aug. 2011.
- [27] A. Mahmood and Y. Kim, "Leader-following formation control of quadcopters with heading synchronization," *Aerosp. Sci. Technol.*, vol. 47, pp. 68–74, Dec. 2015.



YUE GAO received the B.S. degree in software engineering from the Beijing Institute of Technology, in 2007, and the M.S. degree in pattern recognition and intelligent system from Beihang University, in 2010. He is currently a Senior Engineer at Space Star Technology Company, Ltd. His research interests include image processing, artificial intelligence, satellite application, and satellite mission planning.



HAO LIU (Member, IEEE) received the B.E. degree in control science and engineering from Northwestern Polytechnical University, Xi'an, China, in 2008, and the Ph.D. degree in automatic control from Tsinghua University, Beijing, China, in 2013. In 2012, he was a Visiting Student with the Research School of Engineering, The Australian National University. Since 2013, he has been with the School of Astronautics, Beihang University, Beijing, where he is currently an Associate Professor. He has also been with The University of Texas at Arlington Research Institute, Fort Worth, TX, USA. His research interests include formation control, reinforcement learning, robust control, nonlinear control, unmanned aerial vehicles, unmanned underwater vehicles, and multiagent systems. He received the Best Paper Award at IEEE ICCA 2018. He serves as an Associate Editor for *Transactions of the Institute of Measurement and Control* and *Advanced Control for Applications: Engineering and Industrial Systems*.



YU TIAN received the B.S. degree in guidance, navigation, and control from Beihang University, Beijing, China, in 2016, where she is currently pursuing the M.E. degree with the School of Astronautics. Her research interests include robust control, nonlinear control, multiagent systems, and satellite flight control.